CDF//TOP/GROUP/11063
January 31, 2014

Search for an Invisible Decaying Higgs Boson in Dilepton Events at CDF

M. Bauce, K. Knoepfel, D. Lucchesi, C. Principato, G. Punzi, C. Vellidis

Abstract

We present the first search at the Tevatron for a Higgs boson decaying to an invisible final state. We use the full CDF Run II data set corresponding to 9.7 fb^{-1} of integrated luminosity. We search in the associated ZH production mode and require two same-flavor, oppositely charged leptons and a significant value of missing transverse energy to be in the final state. We exclude values of $\sigma_{ZH\times\mathcal{B}(H\to\text{invisible})}$ greater than 90 fb at 95% credibility level for a Higgs boson mass of 125 GeV/c^2. We perform this analysis across a Higgs boson mass range of 115 to 150 GeV/c^2. We are able to exclude a $\mathcal{B}\,(H \to \text{invisible}) = 100\%$ assumption at Higgs boson masses lower than 120 GeV/c^2.

Contents

1 Introduction

Even with the discovery of a Higgs boson, physicists know that the Standard Model of particle physics cannot be the final answer since it has known shortcomings. For example, it fails to provide an explanation for dark matter or why the masses of fundamental particles such as electrons and muons are so different. This is the reason why the future steps are checking its details and determining as well as possible whether it is or isn't precisely what is predicted by the Standard Model. The Higgs Boson is the last discovered particle of the Standard Model of Particle Physics. The Higgs Boson is a manifestation of the Higgs mechanism through which all fundamental particles are thought to acquire their mass. The Higgs field gives mass to all of the known apparently−elementary massive particles: quarks, charged leptons, W and Z particle, and even the neutrinos. The only particles it leaves alone are the gluons and the photon (and the presumed graviton). This is all very well understood within the equations of the Standard Model of particle physics, which describe all of these particles and their fields. It's clear from those equations that it is impossible for any of these particles to be massive if there isn't some kind of Higgs field around. As a consequence of all of this, the Higgs particle interacts directly with the known particles with a strength related to their masses. And consequently it decays to pairs of these particles (more precisely, to a particle and its antiparticle) with a rate that is related to their masses, as long as the interaction is direct. Roughly speaking, decays to heavy particles are more likely than those to lightweight particles, though there are caveats to come.

About 5% of Higgs particles are expected to be produced along with a W or Z particle. About 22% of the time, a W particle will decay to a lightweight charged lepton (more precisely, to an electron, positron, muon or anti−muon), which, if it is energetic enough, will usually be recognized by the trigger system as a good reason to store the data from the corresponding bunch−crossing in which it appears. Similarly, 6% of Z particles decay to an electron−positron pair or a muon−antimuon pair, and these will usually be stored. In these cases, the decision to store the bunch−crossing is completely independent of how the Higgs particle itself decays. No matter how crazy and untriggerable is the Higgs decay, the decay of the W or Z in these collisions will assure the data from about 1% of the exotic Higgs decays will be recorded. Higgs decay modes are given in Figure [1].

Subsequent decays of the Z boson to electron and muon pairs provide the

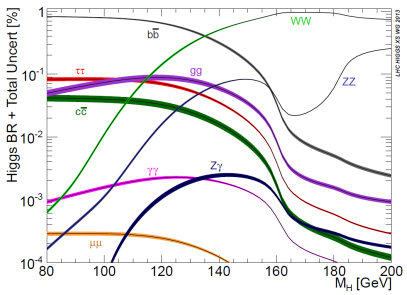

Figure 1: The plot display the branching of the Standard Model Higgs boson to known particles as a function of the mass. Font: LHC HIGGS XS WG 2013

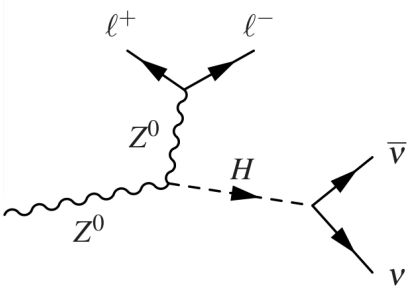

Figure 2: Feynman diagram of ZH process.

cleanest signatures for detection at hadron collider experiments because of the very small expected background, as shown in Figure [1].
Other processes that does not involve the Higgs can also result in a two lepton plus $\not{E}_T$final state. In particular Diboson ZZ production is the dominant process: $ZZ \to ll\nu\nu$ where both bosons decay leptonically. The simplest H →invisible process is highly suppressed in the SM. However, beyond-the-SM scenarios allow for enhanced H →invisible decay rates that are potentially observable by collider experiments. In this analysis, we search for a H →invisible process in the ZH associated production mode. Despite the suppressed cross section relative to gluon fusion, the ZH production mode allows one to trigger on leptonic decays of the Z. For this analysis, we reconstruct Z candidates by combining e^+e^- and $\mu^+\mu^-$ dilepton four-momenta. We do not explicitly reconstruct $Z \to \tau^+\tau^-$ processes, but as we are not able to infer the missing energy from neutrinos, we gain some acceptance from $\tau^+\tau^-$ decays to same-flavor final states. Events with $e^\pm\mu^\mp$ pairs are used as a

control region to test background modeling, as well as events with same-sign, same-flavor lepton pairs. The event selection is described below.

2 Lepton Selection

The lepton categories used in this analysis are:

- Electron: TCE, LBE, PHX
- Muon: CMUP, CMX, CMIoCES, CMIoPES and the new categories CMP,MsKs,BMU.
- Track: CrkTrk

The selection cuts, the efficiency scale factor determination procedures and the fake rate calculations are the same described in CDF note 8538 [1].

3 Event Selection

To measure the ZH cross section in the $ll\nu\nu$ decay channel we apply a similar strategy to the one applied in the analysis [2]. We start selecting one $Z \to ll$ in the detector, then we try to get indirect information about $H \to \nu\nu$ from the unbalance in the detector transverse plane. The two undetected neutrinos should result in a significant $\not\!\!E_T$in the final state. From the sample of events collected with the single high$-p_T$ triggers we select events containing exactly two isolated leptons, belonging to one of the lepton categories listed in Section 2. The leptons are required to have $p_T \geq 45\text{GeV}/c$.
To reconstruct the $Z \to ll$ decay we require that the two leptons form a same favor and opposite charge pair $(e^+e^-, \mu^+\mu^-)$ with $76 \leq M_{ll} \leq 106\frac{GeV}{c^2}$. These requirements have only a marginal acceptance on $Z \to \tau\tau$ production which is included in this analysis only when both τs decay to e or μ satisfying the other kinematic requirements.

These requirements define a preselected sample of dilepton events dominated by the single Z production $(Drell - Yan)$ which is predicted to be produced with a cross section of $\approx 490pb$ for m$(ll) \geq 20\frac{GeV}{c^2}$ at NNLo. The main difference between $ZH \to ll\nu\nu$ signal and the $Drell-Yan$ background are the two additionally produced neutrinos in the final state. While in ZH production these should appear as a significant $\not\!\!E_T$in the detector, the

$Drell - Yan$ background can present (even large) due to instrumental effect. In order to eliminate the Drell-Yan background we require to have a $\not\!\!E_T \geq 60 GeV$.
These requirements define a preselected sample of dilepton events dominated by the $ZZ \to ll\nu\nu$.
The main difference between $ZH \to ll\nu\nu$ signal and the $ZZ \to ll\nu\nu$ background is the kinematic of the decaying leptons. In the preselected sample we have additional contribution also from other diboson processes, $WW \to l\nu l\nu$ and $WZ \to l\nu l'l'$, that has both similar leptonic decay modes.

An additional small contribution comes from $W\gamma$ and W+jets production, where a photon or a jet can mimic the second lepton in the final state. At last, $t\bar{t}$ production can give a dileptonic signature (when $t\bar{t} \to (W \to l\nu)\, b\, (W \to l\nu) b$) associated with a large hadronic activity in the calorimeters.

We model the kinematic of the ZH signal and of the several background processes using Monte Carlo (MC) simulations. The generator used, the predicted theoretical cross section, and the names of the dataset used are the same of the 10954 note. In this analysis the MC samples are normalized so as to reproduce the expected number of events in the considered integrated luminosity. The normalization of the $Drell - Yan$ simulated sample will be extracted from a fit to the data in a control sample kinematically similar to the one considered for the measurement.

The contribution from W+jets production with the misidentified jet mimicking one of the two leptons is evaluated from a sample of jet−triggered data with the fake rate method[1]. In this case we consider only events with one real lepton and the possible fake second lepton. The events containing one real lepton and two candidate fake leptons are splitted and two lepton+fake candidate events are considered. Each candidate is weighted with the appropriate fake rate and added to the background prediction. Particular attention is given to the reconstructed $Z \to ll$ properties, i.e. the two lepton transverse momenta, the opening angles between the two leptons ($\Delta\phi(ll)$, $\Delta R(ll)$), the reconstructed Z mass (M_{ll}) and transverse momentum of the dilepton system ($p_T{}^Z$). In addition we check the modeling of some other global variables (N_{jets}, $\not\!\!E_T$) for these events. The data−to−MC comparison shows some disagreement that are due to intrinsic problems in the Drell−Yan MC simulation. These will not have a dramatic effect on the analysis since we will try to reduce the contribution from this process cutting on $\not\!\!E_T$. The Drell−Yan contribution in the final signal region will be extracted from a fit to the data in an orthogonal control region; the uncertainty extracted from

the fit will be included as systematic uncertainty considered for the cross section measurement. In order to extract the $ZH \to ll\nu\nu$ signal from the background dominated sample we exploit some kinematic properties of the reconstructed event. At first, since we don't expect $ll\nu\nu$ events to have a large hadronic activity, we apply a veto on the presence of a $Z-$recoiling jet: we practically reject events that have any jet ($E_T \geq 15GeV$, L5 corr.) with $\Delta\phi(j, Z) \geq \frac{\pi}{2}$. In the Drell$-$Yan background events (as well as W+jets) is often present a $high - E_T$ jet recoiling against the $Z \to ll$, hence this veto reduces this contribution while doesn't affect significantly the ZH signal. The veto applied select a sample composed for its $\approx 98\%$ by events with no reconstructed jet at all, still dominated by Drell$-$Yan events. To reduce the background and isolate ZH events we exploit indirect information on the additional Z decaying to a pair of neutrinos. In $ZH \to ll\nu\nu$ signal we expect to observe a significant amount of $\not\!\!E_T$due to the two undetected neutrinos, while single produced Z events should eventually present $\not\!\!E_T$due mainly to detector resolution and instrumental effects. To further improve the signal-to-background ratio in the considered data sample and prevent from detector resolution mismodeling effects we require that the observed $\not\!\!E_T$is

$$MET \geq 60\, GeV \tag{1}$$

In summary in order to study this process events are collected using $high-p_T$ muon, $high-E_T$ electron and Met+Pem triggers, using a dataset corresponding to 9.7 fb^{-1} of CDF data.

4 Signal Region

We define a Signal Region for this measurement selecting events passing the following requirements:
In order to reconstruct the $Z \to ll$ event the following features are requested:

- Exactely two Same Flavor and opposite Charge leptons
- Reconstructed invariant mass: $82 \leq M_{ll} \leq\ 100GeV/c^2$
- Different reconstructed lepton categories for electrons, muons and high$-$quality tracks

Events are required to be boosted in order to account of the recoil against the Higgs boson:

- Consider as a signal region $p_T(ll) \geq 45\, GeV$
- $30 \leq p_T(ll) \leq 45\, GeV$ events considered as a control sample

In order to reduce spurious background boosted events that have $\not\!\!E_T$and level 5 correction:

- No jets reconstructed that have $E_T \geq 15\, GeV$ and L5 corrections, with $\Delta\phi \geq 2.0$ from the Z

Events $ZH \to ll\nu\nu$ are searched in the tail of the $\not\!\!E_T$distribution
Features ($\epsilon_{ID}, \epsilon_{trig}$, etc) and tools from ZZ cross section measurement and $H \to WW$ search.

Tables show the event selection for each sample during each stage of the analysis after the skim. We only present efficiencies for the signal region event selection.

	Z+jets		
Description	$Z \to e^+e^-$	$Z \to \mu^+\mu^-$	$Z \to \tau^+\tau^-$
Events after skim	434739	709579	12025
Cut 1 (dileptonType $\neq$ -1)	1	1	1
Cut 2 (dileptonFlavor $\neq$ kflav_ em | kflav_ etau | | kflav_ mtau)	0.99	0.99	0.58
Cut 3 (dileptonType $\neq$ k_ PHX_ PHX | | k_ PHX_ PLBE | | k_ PLBE_ PLBE)	0.99	0.98	0.96
Cut 4 (N_{jcAw} <0.)	0.78	0.79	0.82
Cut 5 ($\Delta\phi(\not\!\!E_T, ll) > 0.5$)	0.67	0.63	0.35
Cut 6 ($Z_{Pt} > 45.$ GeV/c)	0.0005	0.0005	0.0002
Cut 7 (82. <dimass < 100. GeV/c^2)	0.73	0.78	0.08
Cut 8 ($\not\!\!E_T$> 60. GeV)	0.02	0.02	0
Cut 9 (cutMask == true)	1	0.95	nan
Cut 10 (SS regions reject PHX)	1	1	nan
Cut 11 (SS regions reject PHX)	1	1	nan
Overall efficiency	$3.36 \cdot 10^{-6}$	$3.18 \cdot 10^{-6}$	
Expected events	1.90	2.25	0.03

Description	W+jets
Events after skim	50331.9
Cut 1 (dileptonType $\neq$ -1)	0.90
Cut 2 (dileptonFlavor $\neq$ kflav_ em | kflav_ etau | | kflav_ mtau)	0.94
Cut 3 (dileptonType $\neq$ k_ PHX_ PHX | | k_ PHX_ PLBE | | k_ PLBE_ PLBE)	0.92
Cut 4 (N_{jcAw} <0.)	0.72
Cut 5 ($\Delta\phi(\not\!\!E_T, ll) > 0.5$)	0.60
Cut 6 ($Z_{Pt} > 45.$ GeV/c)	0.02
Cut 7 (82. <dimass < 100. GeV/c^2)	0.10
Cut 8 ($\not\!\!E_T$> 60. GeV)	0.33
Cut 9 (cutMask == true)	0.31
Cut 10 (SS regions reject PHX)	1
Cut 11 (SS regions reject PHX)	1
Overall efficiency	$7.56 \cdot 10^{-5}$
Expected events	3.8 ± 0.6

	$W\gamma$		
Description	$W \to e + \nu$	$W \to \mu + \nu$	$W \to \tau + \nu$
Events after skim	1041.1	695.81	65.86
Cut 1 (dileptonType $\neq$ -1)	1	1	1
Cut 2 (dileptonFlavor $\neq$ kflav_ em | kflav_ etau | | kflav_ mtau)	0.99	0.14	0.60
Cut 3 (dileptonType $\neq$ k_ PHX_ PHX | | k_ PHX_ PLBE | | k_ PLBE_ PLBE)	0.75	0.99	0.85
Cut 4 (N_{jcAw} <0.)	0.85	0.85	0.82
Cut 5 ($\Delta\phi(\not\!\!E_T, ll) > 0.5$)	0.92	0.93	0.86
Cut 6 ($Z_{Pt} > 45.$ GeV/c)	0.11	0.12	0.10
Cut 7 (82. <dimass < 100. GeV/c^2)	0.07	0.08	0.11
Cut 8 ($\not\!\!E_T$> 60. GeV)	0.18	0.26	0.35
Cut 9 (cutMask == true)	0.30	0.67	0.68
Cut 10 (SS regions reject PHX)	1	1	1
Cut 11 (SS regions reject PHX)	1	1	1
Overall efficiency	$2.68 \cdot 10^{-4}$	$1.84 \cdot 10^{-4}$	$9.38 \cdot 10^{-4}$
Expected events	0.28 ± 0.01	0.13 ± 0.02	0.06
Tot. Expected Events	0.5 ± 0.1		

Description	$t\bar{t}$
Events after skim	1250.12
Cut 1 (dileptonType $\neq$ -1)	1
Cut 2 (dileptonFlavor $\neq$ kflav_ em | kflav_ etau | | kflav_ mtau)	0.61
Cut 3 (dileptonType $\neq$ k_ PHX_ PHX | | k_ PHX_ PLBE | | k_ PLBE_ PLBE)	0.98
Cut 4 (N_{jeAw} <0.)	0.17
Cut 5 ($\Delta\phi(\not\!\!E_T,ll) > 0.5$)	0.81
Cut 6 ($Z_{Pt} > 45.$ GeV/c)	0.52
Cut 7 (82. <dimass < 100. GeV/c^2)	0.12
Cut 8 ($\not\!\!E_T$> 60. GeV)	0.87
Cut 9 (cutMask == true)	0.97
Cut 10 (SS regions reject PHX)	1
Cut 11 (SS regions reject PHX)	1
Overall efficiency	$4.36 \cdot 10^{-3}$
Expected events	5.5 ± 0.9

Description	WZ
Events after skim	733.75
Cut 1 (dileptonType $\neq$ -1)	0.99
Cut 2 (dileptonFlavor $\neq$ kflav_ em | kflav_ etau | | kflav_ mtau)	0.90
Cut 3 (dileptonType $\neq$ k_ PHX_ PHX | | k_ PHX_ PLBE | | k_ PLBE_ PLBE)	0.97
Cut 4 (N_{jeAw} <0.)	0.31
Cut 5 ($\Delta\phi(\not\!\!E_T,ll) > 0.5$)	0.77
Cut 6 ($Z_{Pt} > 45.$ GeV/c)	0.43
Cut 7 (82. <dimass < 100. GeV/c^2)	0.44
Cut 8 ($\not\!\!E_T$> 60. GeV)	0.58
Cut 9 (cutMask == true)	0.83
Cut 10 (SS regions reject PHX)	1
Cut 11 (SS regions reject PHX)	1
Overall efficiency	$1.86 \cdot 10^{-2}$
Expected events	13.7 ± 1.5

Description	WW
Events after skim	1969.84
Cut 1 (dileptonType $\neq$ -1)	1
Cut 2 (dileptonFlavor $\neq$ kflav_ em | kflav_ etau | | kflav_ mtau)	0.60
Cut 3 (dileptonType $\neq$ k_ PHX_ PHX | | k_ PHX_ PLBE | | k_ PLBE_ PLBE)	0.97
Cut 4 (N_{jeAw} <0.)	0.83
Cut 5 ($\Delta\phi(\not\!\!E_T,ll) > 0.5$)	0.90
Cut 6 ($Z_{Pt} > 45.$ GeV/c)	0.41
Cut 7 (82. <dimass < 100. GeV/c^2)	0.11
Cut 8 ($\not\!\!E_T$> 60. GeV)	0.52
Cut 9 (cutMask == true)	0.96
Cut 10 (SS regions reject PHX)	1
Cut 11 (SS regions reject PHX)	1
Overall efficiency	$9.76 \cdot 10^{-3}$
Expected events	19.2 ± 1.8

Description	ZZ
Events after skim	569.26
Cut 1 (dileptonType $\neq$ -1)	0.99
Cut 2 (dileptonFlavor $\neq$ kflav_ em | kflav_ etau | | kflav_ mtau)	0.97
Cut 3 (dileptonType $\neq$ k_ PHX_ PHX | | k_ PHX_ PLBE | | k_ PLBE_ PLBE)	0.98
Cut 4 (N_{jeAw} <0.)	0.27
Cut 5 ($\Delta\phi(\not\!\!E_T,ll) > 0.5$)	0.77
Cut 6 ($Z_{Pt} > 45.$ GeV/c)	0.46
Cut 7 (82. <dimass < 100. GeV/c^2)	0.75
Cut 8 ($\not\!\!E_T$> 60. GeV)	0.71
Cut 9 (cutMask == true)	0.96
Cut 10 (SS regions reject PHX)	1
Cut 11 (SS regions reject PHX)	1
Overall efficiency	$4.77 \cdot 10^{-2}$
Expected events	27.2 ± 2.9

Description	ZH $m_H = 125$ GeV/c^2
Events after skim	20.60
Cut 1 (dileptonType $\neq$ -1)	1
Cut 2 (dileptonFlavor $\neq$ kflav_ em | kflav_ etau | | kflav_ mtau)	0.99
Cut 3 (dileptonType $\neq$ k_ PHX_ PHX | | k_ PHX_ PLBE | | k_ PLBE_ PLBE)	0.98
Cut 4 (N_{jeAw} <0.)	0.85
Cut 5 ($\Delta\phi(\not\!\!E_T,ll) > 0.5$)	0.91
Cut 6 ($Z_{Pt} > 45.$ GeV/c)	0.75
Cut 7 (82. <dimass < 100. GeV/c^2)	0.85
Cut 8 ($\not\!\!E_T$> 60. GeV)	0.85
Cut 9 (cutMask == true)	0.96
Cut 10 (SS regions reject PHX)	1
Cut 11 (SS regions reject PHX)	1
Overall efficiency	0.40
Expected events	8.17

Description	Data
Events after skim	$1.42 \cdot 10^6$
Cut 1 (dileptonType $\neq$ -1)	0.97
Cut 2 (dileptonFlavor $\neq$ kflav_ em | kflav_ etau | | kflav_ mtau)	0.99
Cut 3 (dileptonType $\neq$ k_ PHX_ PHX | | k_ PHX_ PLBE | | k_ PLBE_ PLBE)	0.95
Cut 4 (N_{jeAw} <0.)	0.80
Cut 5 ($\Delta\phi(\not\!\!E_T,ll) > 0.5$)	0.64
Cut 6 ($Z_{Pt} > 45.$ GeV/c)	0.003
Cut 7 (82. <dimass < 100. GeV/c^2)	0.34
Cut 8 ($\not\!\!E_T$> 60. GeV)	0.16
Cut 9 (cutMask == true)	0.78
Cut 10 (SS regions reject PHX)	1
Cut 11 (SS regions reject PHX)	1
Overall efficiency	$5.49 \cdot 10^{-5}$
Expected events	78

The expected contribution for the signal and background processes are obtained using the MC simulation described in Table [1] and the data−driven method for the W+jets contribution.

Table 1: Number of predicted and observed events in the Signal Region defined by no recoiling jets, $82 \leq M_{ll} \leq 100 GeV/c^2$, $\Delta\phi(MET, l) \geq 2.0$, $\not\!\!E_T \geq 60 GeV$

$ZH \rightarrow \ell^+\ell^- +$ **invisible** (signal region) CDF Run II Preliminary, $\mathcal{L} = 9.7$ fb^{-1}	
Z +jets	7.1 ± 3.1
$W+$ jets	3.8 ± 0.6
$W\gamma$	0.5 ± 0.1
$t\bar{t}$	5.5 ± 0.9
WZ	13.7 ± 1.5
WW	19.2 ± 1.8
ZZ	27.2 ± 2.9
Total prediction	76.9 ± 7.2
ZH ($m_H = 125$ GeV/c^2)	8.2 ± 1.3
Data	78

Given the mismodeling in Drell−Yan reproduction observed in the dilepton inclusive sample we extract the normalization of this process from an $e - \mu$ orthogonal sample with the kinematic properties similar to the SR considered. We fit the normalization of the Drell−Yan component from the $\not\!\!E_T \leq 60 GeV$ distribution of the data in the Signal Region, as a scale factor with respect to the nominal MC normalization, and apply the same one to scale the Drell−Yan contribution in the SR. The fit result in a correction factor

$$k = 1.7 \pm 0.5\% \times \textit{the nominal MC normalization} \tag{2}$$

To reach a better agreement between data and MonteCarlo simulation we shifted the $\not\!\!E_T$distribution in the Signal Region by a factor of $+3 \pm 33\%$ GeV. Table [1] shows the expected and observed number of events in the Signal Region in the full CDF dataset considered ($L = 9.7$fb^{-1}) where we can see that

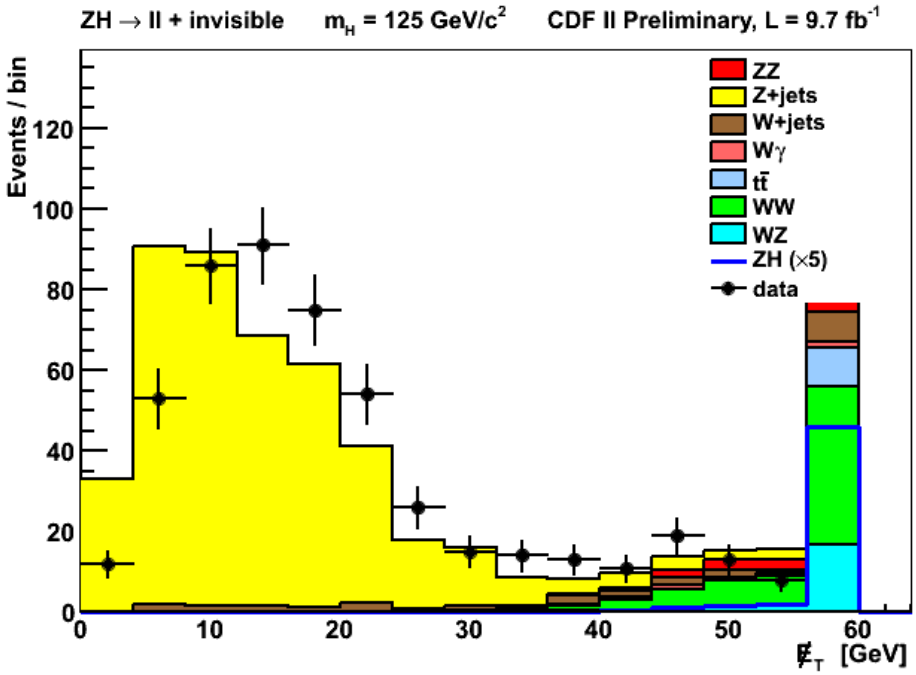

the sample is dominated by ZZ, and WW contributions, with significant WZ and Drell-Yan signal contributions. Figures [2] show the comparison between data and MC for the kinematic variables distribution that charachterize the events in the Signal Region.

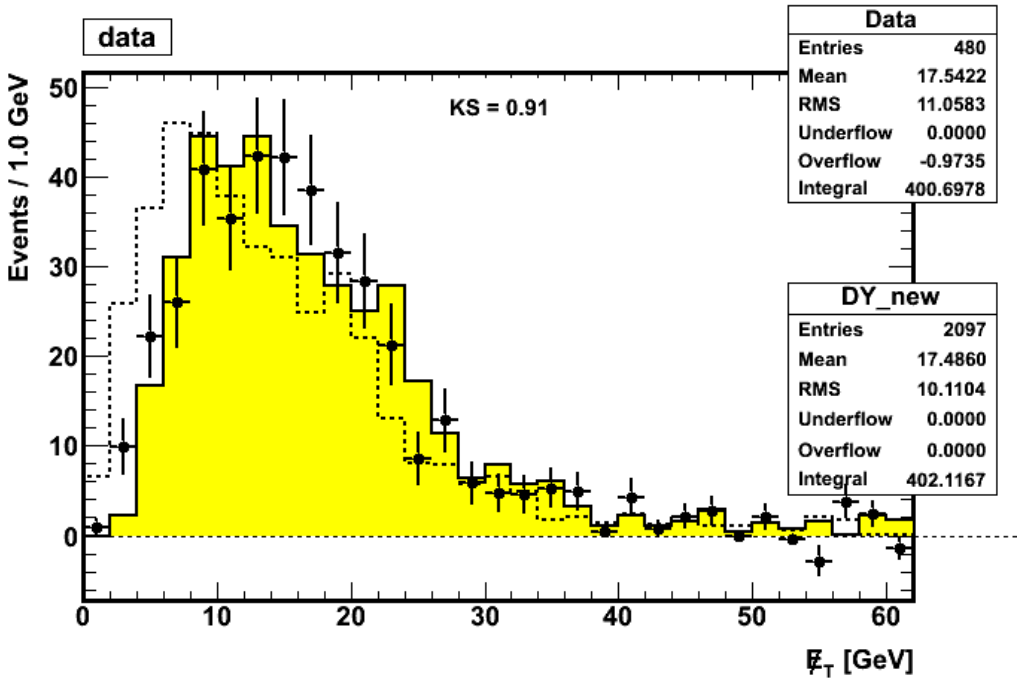

5 Background Modeling

The dominant background contributions in the previously defined Signal Region are due to ZZ and WW, which present similar signature in the final state but higher production cross section than ZH. WW production is kinematically similar to the ZZ diboson one, hence we would like to be able to model it fairly, exploiting a full Next-to-Leading order simulation. Drell-Yan residual contribution is mainly characterized by the presence of $\not\!\!E_T$ which doesn't reflect the production of undetected particles, mostly due to detector resolution effect, which is not trivial to model in the MC simulation. These background processes are tested in non-overlapping data sample of events:

- $e - \mu$ sample
- Same Sign sample
- Side Bands sample

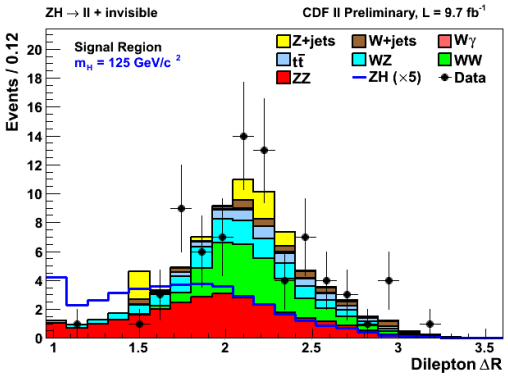

(a) $\Delta R(ll)$ between leptons

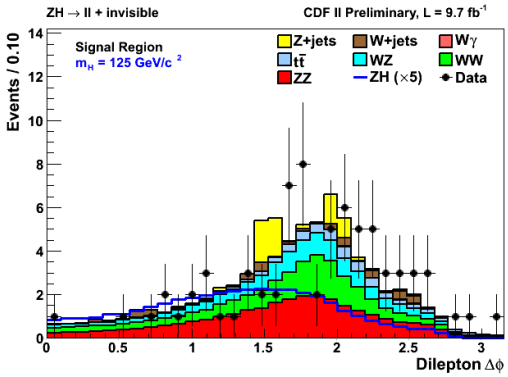

(b) $\Delta\phi(ll)$ between leptons

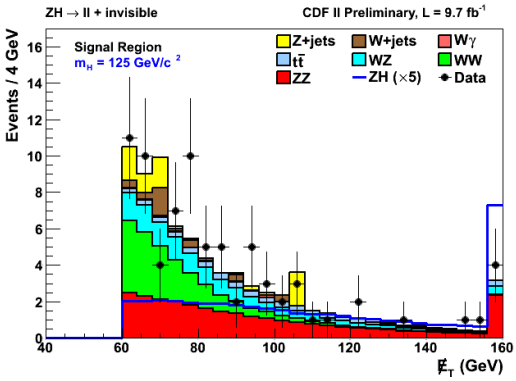

(c) Missing Transverse Energy

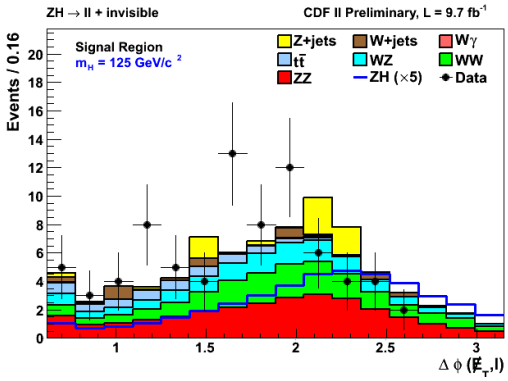

(d) $\Delta\phi$ between $\not\!\!E_T$and leading lepton

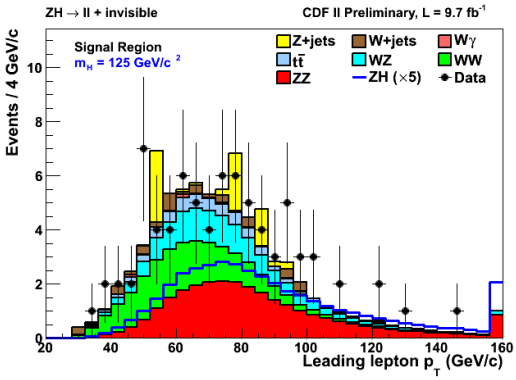

(e) Transverse momentum of leading lepton

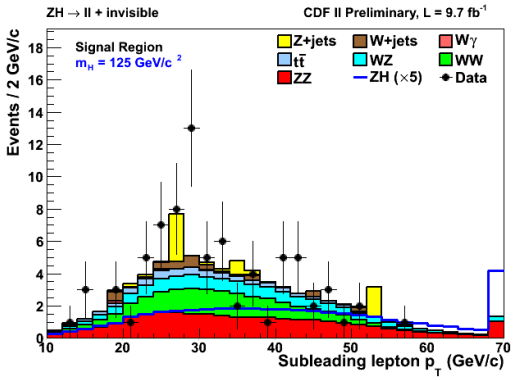

(f) Transverse momentum of subleading lepton

Figure 3: Signal region

5.1 $e - \mu$ Control Region

To test the WW modeling in a kinematic region similar to the Signal Region we select events with two isolated leptons in the final state of different flavor, i.e. $e^{\pm}, \mu^{\mp}$, satysfing all the requirements that define the Signal Region, but a different dilepton invariant mass range. Selecting different flavor leptons we drastically reduce contribution from real Z. A residual contribution of Drell-Yan events come from $Z \to \tau\tau$ decays with subsequent leptonic decays of the τs that can produce an $e - \mu$ pair. Since in this case the two leptons don't necessarily come from a Z we broaden the range of the considered dilepton mass spectrum, to increase the statistic of the control sample and modify the Signal Region requirement as follow:

- $40 \leq M_{e\mu} \leq 140 GeV/c^2$

This CR is used also to evaluate from data the proper normalization of the Drell-Yan background contribution in a kinematic region with large $\not\!\!E_T$, hence similar to the Signal Region. We do that considering the ΔR kinematic distribution and comparing simulation for the several processes to data. Fitting the Drell-Yan component to data in this control sample we obtain a correction k= $1.7 \pm 0.5x$ the MC nominal normalization.
This correction factor applied to the Drell-Yan simulation improve significantly the agreement between data and simulation in this CR and is applied also to obtain the proper normalization for the Drell-Yan contribution in the Signal Region.

Table [2] summarizes the number of events expected from the several processes and the yields in the collected data. The most relevant kinematic variable distributions of the events in the $e - \mu$ Control Region for data and Monte Carlo are shown in Figures [3]. No significant discrepancy is noticeable in the data-to-simulation comparison, with uncertainties dominated by the limited statistics of the sample considered. once tested in this sample, we can assume that the simulation properly models the WW background also in the Signal Region.

Table 2: Number of predicted and observed events in the $e\mu$ Control Region defined by an $e^{\pm}\,\mu^{\mp}$ pair, no jet with $E_T \geq 15\,GeV$ with $\Delta\phi(Z, J) \geq 2.0$ rad, $40 \leq M_{ll} \leq 140 GeV/c^2$, $\Delta\phi(MET, l) \geq 0.5$ rad, $\not\!\!E_T \geq 60 GeV$

$\boldsymbol{ZH \to \ell^+\ell^- +}$ **invisible** ($e^{\pm}\mu^{\mp}$ control region) CDF Run II Preliminary, $\mathcal{L} = 9.7$ fb^{-1}	
Z +jets	9.3 ± 4.1
W+ jets	24.2 ± 3.6
$W\gamma$	16.9 ± 2.8
$t\bar{t}$	14.2 ± 2.3
WZ	2.4 ± 0.3
WW	96.4 ± 8.9
ZZ	0.17 ± 0.02
Total prediction	163.7 ± 12.6
Data	155

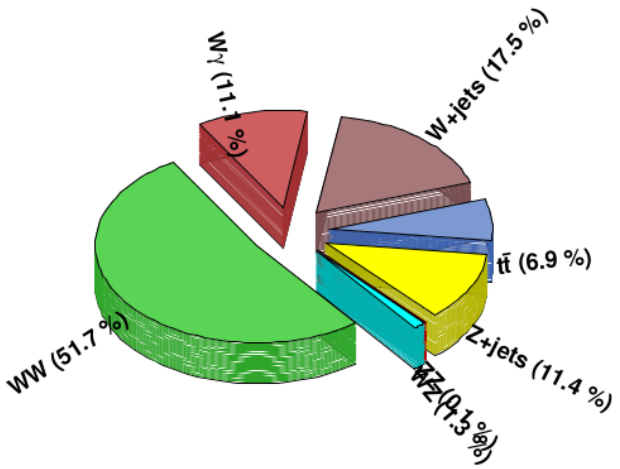

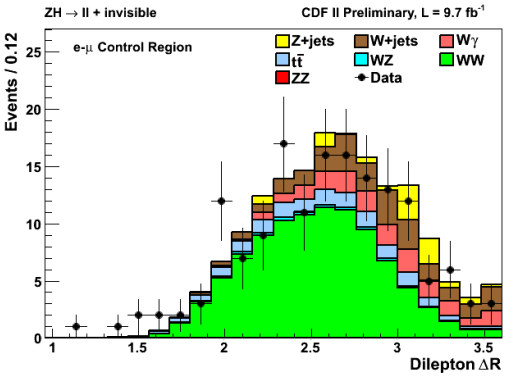

(a) $\Delta R(ll)$ between leptons

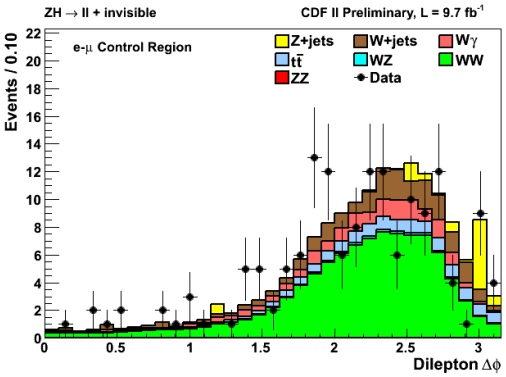

(b) $\Delta\phi(ll)$ between leptons

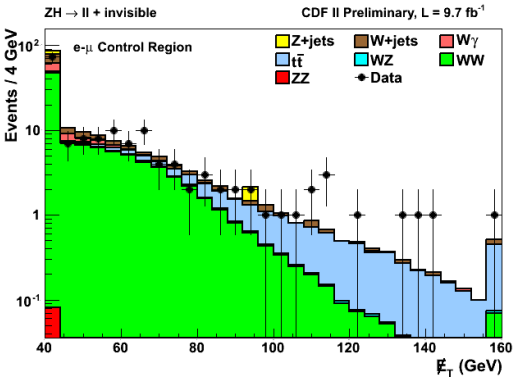

(c) Missing Transverse Energy

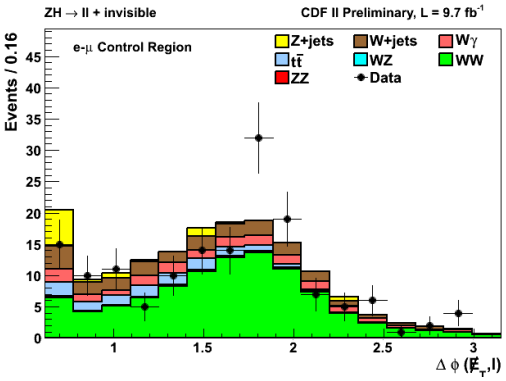

(d) $\Delta\phi$ between $\not\!\!E_T$ and leading lepton

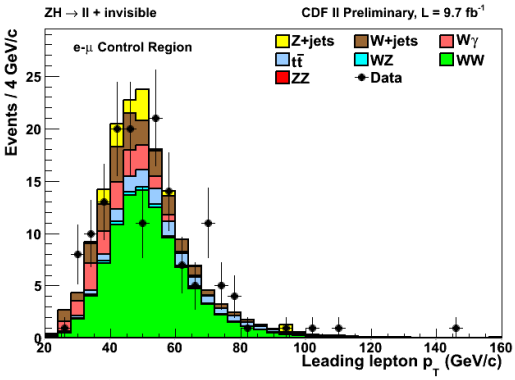

(e) Transverse momentum of leading lepton

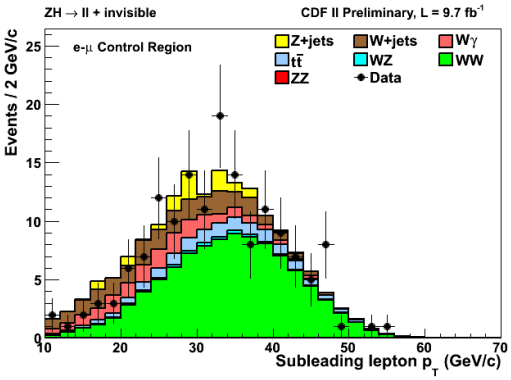

(f) Transverse momentum of subleading lepton

Figure 4: Opposite-flavor, opposite-sign control region

5.2 Same Sign Control Region

To test the W+jets modeling in a kinematic region similar to the Signal Region we select events with two isolated leptons in the final state of same sign, i.e. $e^{\pm}e^{\pm}, \mu^{\pm}\mu^{\pm}$, satysfing all the requirements that define the Signal Region, but a broader dilepton invariant mass range. Selecting same flavor leptons we drastically reduce contribution from real Z. Since in this case the two leptons don't necessarily come from a Z we broaden the range of the considered dilepton mass spectrum, to increase the statistic of the control sample and modify the Signal Region requirements as follow:

- Same Charge and Same Flavor lepton pair
- $40 \leq M_{ll} \leq 140 GeV/c^2$
- $\not\!\!E_T \geq$ 60 GeV
- No jet with $E_T \geq 15 GeV$ (L5 corrections) with $\Delta\phi(Z, j) \geq 2.0 rad$
- min$\Delta\phi(\not\!\!E_T, l) \geq 0.5$ rad

Table 3: Number of predicted and observed events in the Same-sign Control Region defined by a $l^{\pm}l^{\pm}$ pair, no jet with $E_T \geq 15 GeV$ with $\Delta\phi(Z, J) \geq 2.0$ rad, $40 \leq M_{ll} \leq 140 GeV/c^2$, $\Delta\phi(MET, l) \geq 0.5$ rad, $\not\!\!E_T \geq 60 GeV$

$\boldsymbol{ZH \to \ell^+\ell^- +}$ **invisible** (same-sign control region) CDF Run II Preliminary, $\mathcal{L} = 9.7$ fb^{-1}	
Z +jets	2.9 ± 1.3
$W + jets$	30.1 ± 4.5
$W\gamma$	8.4 ± 1.4
$t\bar{t}$	0.22 ± 0.04
WZ	7.2 ± 0.8
WW	1.7 ± 0.2
ZZ	0.66 ± 0.07
Total prediction	51.1 ± 5.1
Data	57

Table [3] summarizes the number of events expected from the several processes and the yields in the collected data. The most relevant kinematic

variable distributions of the events in the Same sign Control Region for data and Monte Carlo are shown in Figures [4]. No significant discrepancy is noticeable in the data-to-simulation comparison, with uncertainties dominated by the limited statistics of the sample considered. Once tested in this sample, we can assume that the simulation properly models the W+jets background also in the Signal Region.

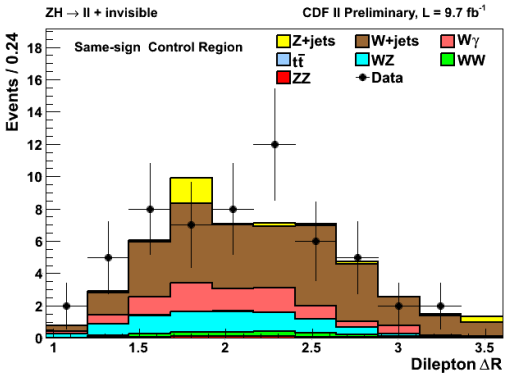

(a) $\Delta R(ll)$ between leptons

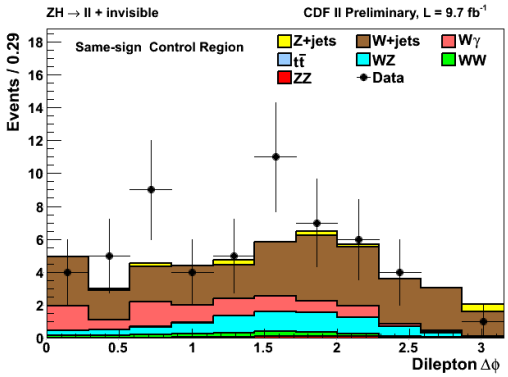

(b) $\Delta\phi(ll)$ between leptons

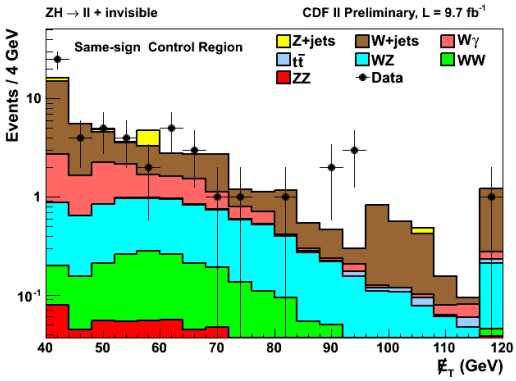

(c) Missing Transverse Energy

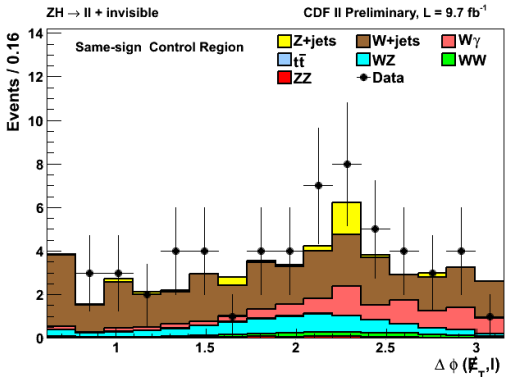

(d) $\Delta\phi$ between $\not\!\!E_T$and leading lepton

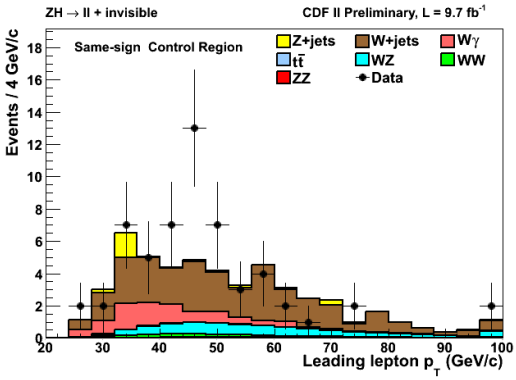

(e) Transverse momentum of leading lepton

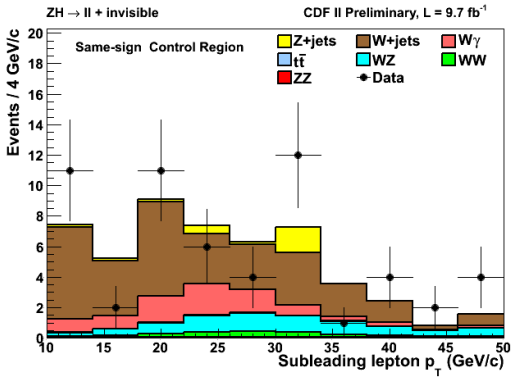

(f) Transverse momentum of subleading lepton

Figure 5: Same-sign, same-flavor control region

Table 4: Number of predicted and observed events in the Side Bands Control Region, e^+e^-, $\mu^+\mu^-$ pair, no jet with $E_T \geq 15\,GeV$ with $\Delta\phi(Z,J) \geq 2.0$ rad, $M_{ll} \in [50,82] \cup [100,132] GeV/c^2$, $\Delta\phi(MET,l) \geq 0.5$ rad, $\not\!\!E_T \geq 50 GeV$

$ZH \rightarrow \ell^+\ell^- +$ **invisible** (sideband control region) CDF Run II Preliminary, $\mathcal{L} = 9.7$ fb^{-1}	
Z +jets	1.7 ± 0.7
$W\ +\ jets$	19.8 ± 3.0
$W\gamma$	6.2 ± 1.0
$t\bar{t}$	20.1 ± 3.3
WZ	5.2 ± 0.6
WW	113.4 ± 10.4
ZZ	6.2 ± 0.7
Total prediction	172.7 ± 13.7
Data	177

5.3 Side Bands Control Region

To test the WW modeling in a kinematic region similar to the Signal Region we select events with two isolated leptons in the final state satysfing all the requirements that define the Signal Region, but in Side Bands mass range. Selecting two leptons with an invariant mass far from the Z-mass we drastically reduce contribution from real Z. We modify the Signal Region requirements as follow:

- Different Charge and Same Flavor lepton pair
- $M_{ll} \in [50,82] \cup [100,132] GeV/c^2$
- $\not\!\!E_T \geq$ 60 GeV
- No jet with $E_T \geq 15 GeV$ (L5 corrections) with $\Delta\phi(Z,j) \geq 2.0 rad$
- min$\Delta\phi(\not\!\!E_T, l) \geq 0.5$ rad

Table [4] summarizes the number of events expected from the several processes and the yields in the collected data. The most relevant kinematic variable distributions of the events in the Side Bands Control Region for data

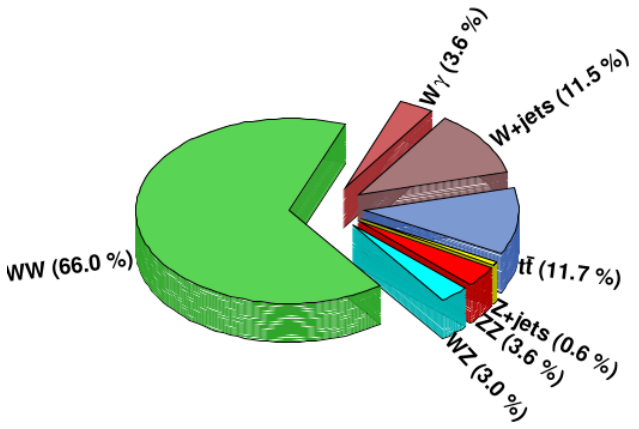

and Monte Carlo are shown in Figures [5]. No significant discrepancy is noticeable in the data-to-simulation comparison, with uncertainties dominated by the limited statistics of the sample considered. Once tested in this sample, we can assume that the simulation properly models the W+jets background also in the Signal Region.

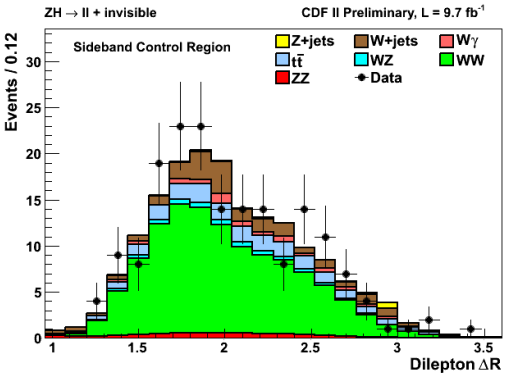

(a) $\Delta R(ll)$ between leptons

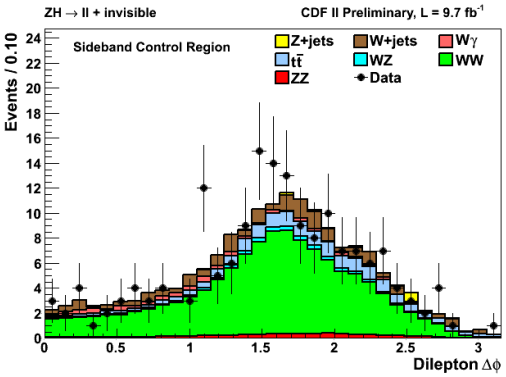

(b) $\Delta\phi(ll)$ between leptons

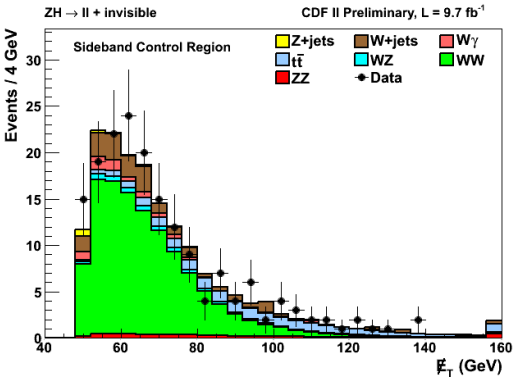

(c) Missing Transverse Energy

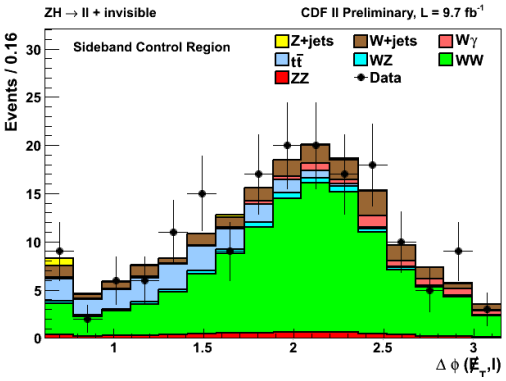

(d) $\Delta\phi$ between $\not\!\!E_T$ and leading lepton

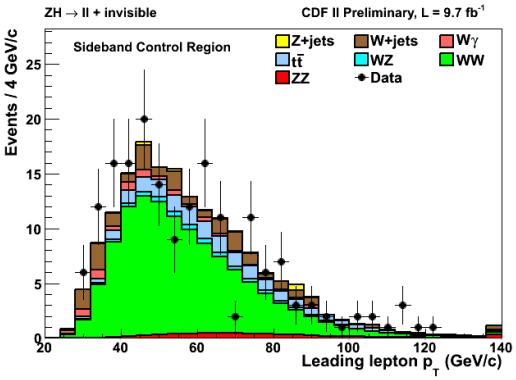

(e) Transverse momentum of leading lepton

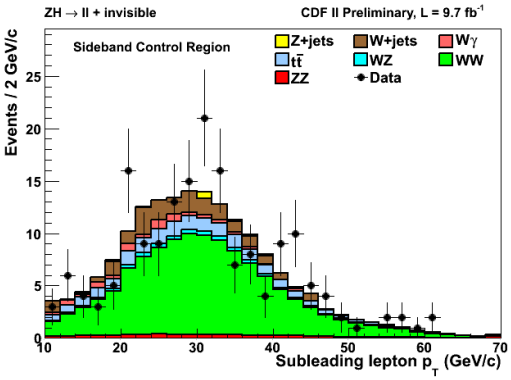

(f) Transverse momentum of subleading lepton

Figure 6: Sideband M_{ll} $[50, 82] \cup [100, 132]\text{GeV}/c^2$ control region

6 dRLeptons Discriminant

We selected as final discriminant the ΔR variable, since the significance of this variable has the highest value between all the kinematic variables we reconstructed, in order to estimate an Upper Limit for the $ZH \rightarrow llvv$ process. In the Figure[6 the kinematic variable distribution of the events for data and Monte Carlo is shown.

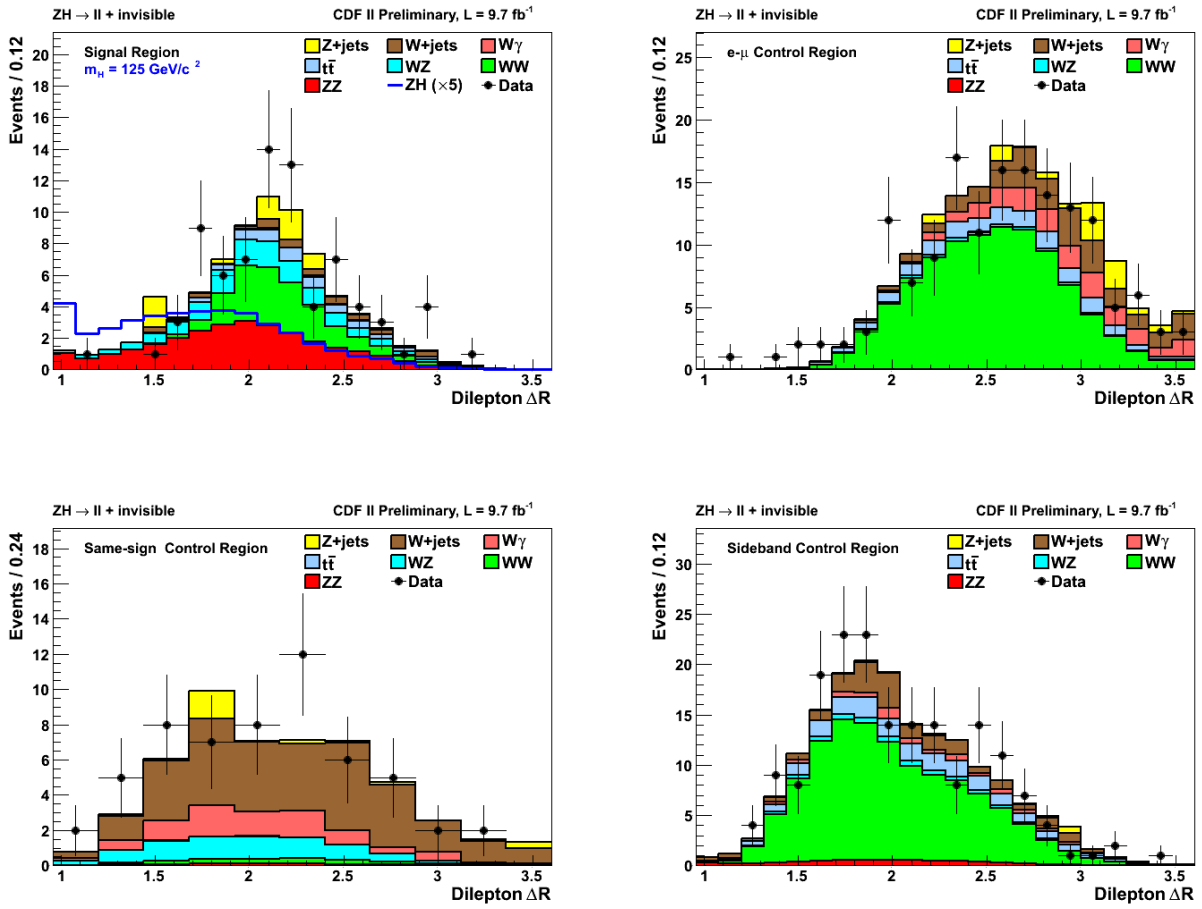

Figure 7: Final Discriminant $\Delta R(ll)$

7 Systematics Uncertainties

Table 5: Table of the Systematic uncertainties considered in the measurement

$ZH \to \ell^+\ell^- +$ **invisible**	CDF Run II Preliminary, $\mathcal{L} = 9.7$ fb^{-1}							
Systematic Uncertainties (%)	ZZ	WZ	WW	$t\bar{t}$	$W + jets$	$Z + jets$	$W\gamma$	ZH
Theory cross section	6	6	6	10		33	10	5
NLO acceptance	5	5		10			5	10
Luminosity	5.9	5.9	5.9	5.9			5.9	5.9
Electron conversion							10	5.9
Jet-energy scale	2	4	1	4		28	3	1
Initial/final state radiation								8
Fake lepton rate					15			
Lepton ID	3	3	3	3		3		3
Trigger efficiency	2	2	2	2		2		2

The systematics uncertainties considered in this analysis are summarized in Table5 and described in detail in the following subsections. The evaluations related to the ZZ and fakes component are the same as those performed for the ZZ cross−section measurement [2].

7.1 Lepton ID Efficiency

Systematic uncertainties due to the lepton ID efficiencies are calculated by coherently varying the lepton ID scale factors by 1σ for each lepton and counting the number of expected events. From a signal MC sample we found a variation of $\pm 3.6\%$ and we take this as the systematic error.

7.2 Trigger Efficiency

Uncertainties from the trigger efficiency are calculated by varying trigger scale factor for the triggerable lepton(s). We found a variation of $\pm 2.1\%$.

7.3 Luminosity

A systematic of ±6% is used on the total luminosity, as suggested from the Joint Physics group.

7.4 Cross Section

The cross−section has been computed at NNLo+NNLL precision with the associated scale and PDF variations following the PDF4LHC prescription.

7.5 NLo Effects on the Acceptance on ZZ production

The Pythia ZZ production Monte Carlo used for acceptances and efficiencies determination is at Lo; using MCFM [9] we calculated the difference in the acceptance due to a full NLo simulation and found it to be ±2.5%, which is assigned as a systematic uncertainty.

7.6 MC $\not{E}_T$modelling uncertainty

There is a reliance on MC to properly model fake $\not{E}_T$. We assign a uncertainty following studies of the Drell−Yan background in $H \to WW$ searches that measure the extent of $\not{E}_T$mis−modelling in MC.

7.7 Fake rates uncertainties

We measure the fake rates in several jet samples and we consider the maximum spread between these measurements as a systematic uncertainty on the background estimation.

8 Results

In $\mathcal{L} = 9.7\text{fb}^{-1}$ of data analyzed we see no evidence of a Higgs boson decaying invisible in the mass range considered so we set a 95%CL upper limit on the Higgs decaying cross section. The limit is obtained using a Bayesian approach, with a likelihood function described in [3], considering all the systematic uncertainties described in Section 7 with the appropriate correlations. The result obtained is shown in Figure[9] and summarized in Table [6].

Table 6: Upper Limits for each mass between $115 \leq m_H \leq 150$ GeV/c^2

$ZH \to \ell^+\ell^- +$ **invisible**	CDF Run II Preliminary, $\mathcal{L} = 9.7$ fb^{-1}					
m_H (GeV/c^2)	95% C.L. on $\sigma_{ZH} \times \mathcal{B}(H \to \text{invisible})/\sigma_{ZH,\text{SM}}$					
	-2 s.d.	-1 s.d.	**Exp.**	+1 s.d.	+2 s.d.	**Obs.**
115	0.73	1.19	**1.82**	2.81	4.37	**0.93**
120	0.79	1.29	**1.97**	3.04	4.78	**0.97**
125	0.84	1.37	**2.10**	3.26	5.08	**1.04**
130	0.90	1.46	**2.23**	3.47	5.47	**1.16**
135	0.95	1.53	**2.35**	3.64	5.77	**1.17**
140	1.03	1.65	**2.52**	3.91	6.18	**1.26**
145	1.09	1.75	**2.67**	4.16	6.64	**1.38**
150	1.15	1.85	**2.82**	4.38	6.97	**1.37**

The limits aren't so stringent in the mass range considered, to significantly improve limits, we need more statistics and luminosities that Tevatron could not deliver.

References

[1] Elliot Lipeles, Mark Neubauer, Shih-Chieh Hsu, Frank Wurthwein *Lepton ID for Multilepton Diboson Analyses*

[2] M. Bauce, D. Lucchesi, with the support of the HWW group, *ZZ cross section measurement in lll'l' and llνν final states using the full CDF dataset*. CDF/PUB/ELECTROWEAK/PUBLIC/10957

[3] T. Junk, *Sensitivity, exclusion and discovery with small signals, large backgrounds, and large systematics (2006).* CDF/DOC/STATISTICS/PUBLIC/8128.

[4] M. Bauce, S. Behari, D. Benjamin, P. Bussey, A. Canepa, B. Carls, S. Carron, M. Casarsa, R. St. Denis, M. d'Errico, P. M. Fernandez, M. Herndon, E. James, S. Jindariani, T. Junk, M. Kruse, A. Limosani, D. Lucchesi, R. Lysak, J. Nett, S. Oh, A. Robson, G. Yu *Search for the SM Higgs in the 4-Lepton Final State using 9.7/fb of data* CDF/PHYS/EXOTIC/CDFR/10770

[5] Elliot Lipeles, Mark Neubauer, Shih-Chieh Hsu, Frank Wurthwein *Lepton ID for Multilepton Diboson Analyses* CDF/PHYS/ELECTROWEAK/CDFR/8538

[6] Kyle J. Knoepfel *Standard Model Higgs Searches at the Tevatron.* CDF/PUB/ELECTROWEAK/PUBLIC/10860

9 Acknowledgments

We thank the Fermilab staff and the technical staffs of the participating institutions for their vital contributions. This work was supported by the U.S. Department of Energy and National Science Foundation; the Italian Istituto Nazionale di Fisica Nucleare; the Ministry of Education, Culture, Sports, Science and Technology of Japan; the Natural Sciences and Engineering Research Council of Canada; the National Science Council of the Republic of China; the Swiss National Science Foundation; the A.P. Sloan Foundation; the Bundesministerium für Bildung und Forschung, Germany; the Korean World Class University Program, the National Research Foundation of Korea; the Science and Technology Facilities Council and the Royal Society, United Kingdom; the Russian Foundation for Basic Research; the Ministerio de Ciencia e Innovación, and Programa Consolider-Ingenio 2010, Spain; the Slovak R&D Agency; the Academy of Finland; the Australian Research Council (ARC); and the EU community Marie Curie Fellowship Contract No. 302103.

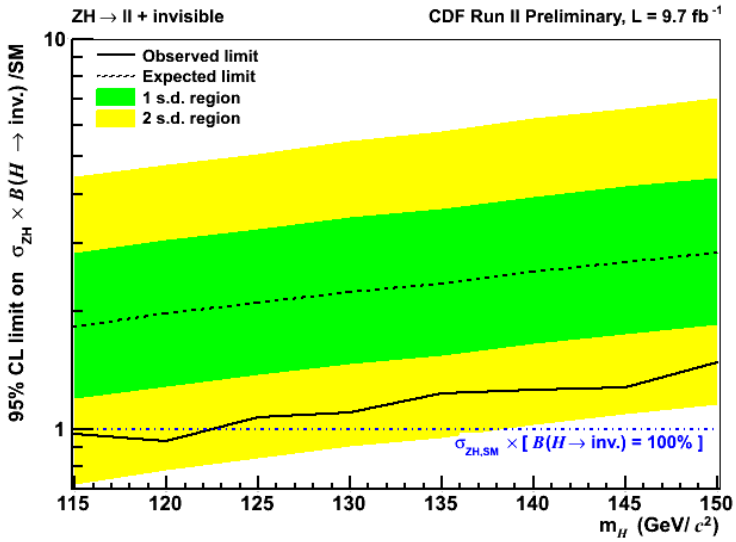

Figure 8: 95% credibility limits for Higgs boson production normalized to the assumed prediction for $\sigma_{ZH,\mathrm{SM}} \times \mathcal{B}(H \rightarrow$ invisible). The branching ratio is assumed to be 100%, whereas the production cross section is assumed to be the SM prediction for ZH production.

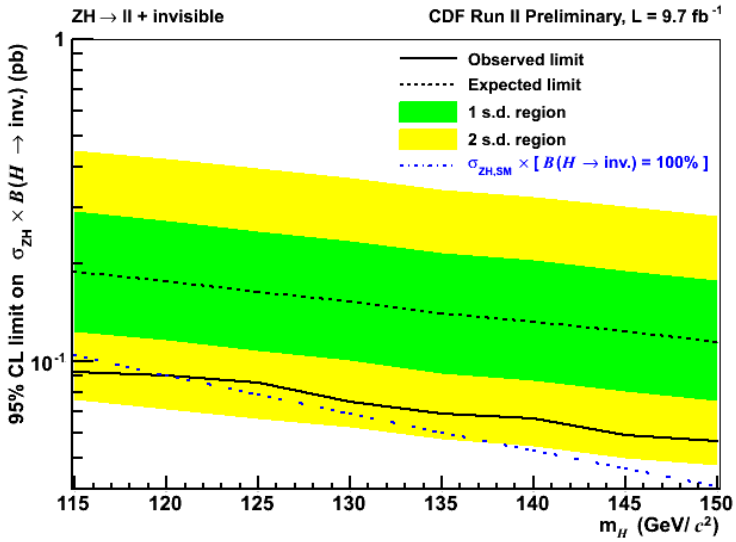

Figure 9: 95% credibility limits for $\sigma_{ZH} \times \mathcal{B}(H \rightarrow$ invisible). No assumption on the cross section or branching ratio is made for the expected and observed results. The SM prediction assuming $H \rightarrow$ invisible branching ratio of 100% is also shown.

Figure 10: 95%CL upper limit on the Higgs decaying cross section